Titanium-catalyzed esterification reactions: beyond Lewis acidity

Wolzak, L.A.; van der Vlugt, J.I.; van den Berg, K.J.; Reek, J.N.H.; Tromp, M.; Korstanje, T.J.

DOI
10.1002/cctc.202000931

Publication date
2020

Document Version
Final published version

Published in
ChemCatChem

Titanium-catalyzed esterification reactions: beyond Lewis acidity

Lukas A. Wolzak,[a] Jarl Ivar van der Vlugt,[b, c] Keimpe J. van den Berg,[d] Joost N. H. Reek,*[b] Moniek Tromp,*[a, e] and Ties J. Korstanje*[a]

Esterification is a key reaction and is used in many synthetic and industrial processes, yet the detailed mechanism of operation of often-used (Lewis acid) catalysts is unknown and subject of little research. Here, we report on mechanistic studies of a titanium aminotriphenolate catalyst, using stoichiometric and catalytic reactions combined with kinetic data and density functional theory (DFT) calculations. While often only the Lewis acidity of the Ti-center is taken into account, we found that the amphoteric nature of this catalyst, combining this Lewis acidity with Brønsted basicity of a Ti-bound and *in situ* formed carboxylate group, is crucial for catalytic activity. Furthermore, hydrogen bonding interactions are essential to pre-organize substrates and to stabilize various intermediates and transition states and thus enhancing the overall catalytic reaction. These findings are not only applicable to this class of catalysts, but could be important for many other esterification catalysts.

Introduction

Esterification is one of the most important reactions in organic synthesis and widely applied in industry, ranging from the production of aspirin to polyesters.[1] Although the direct, uncatalyzed transformation of a carboxylic acid and an alcohol to an ester is possible, it requires temperatures up to 250 °C to achieve full conversion under equilibrium conditions.[1]

As early as 1895, Fischer and Speier described the first catalytic esterification reaction using sulfuric acid as a strong Brønsted acid.[2] In general, for Brønsted acid catalyzed esterification the active species is the protonated carboxylic acid and nucleophilic attack by the alcohol and water formation are the rate limiting steps.[3] Despite being very effective esterification catalysts, strong Brønsted acids also give rise to unwanted side reactions such as the dehydrative etherification of alcohols. The activation of the carbonyl function of the carboxylic acid substrate and subsequent nucleophilic attack by the alcohol onto the electron-deficient carbonyl carbon can also be promoted by Lewis acidic metal ions (Scheme 1), which typically allow for milder reaction conditions and a wider substrate scope.[4–9] As such, recent developments in esterification catalysis have relied heavily on optimizing the Lewis acidity of the metal center.[10–14]

This does, however, not need to be the sole factor that controls activity, as mildly Lewis acidic metal alkoxides, carboxylates, and oxides are also active esterification catalysts.[15,16] Mechanistic proposals that take other factors besides Lewis acidity into account are scarce. Hydrogen bonding interactions between the hydroxyl group of the carboxylic acid and a Lewis basic oxygen bound to the metal center have been proposed, but only in a qualitative description of the reaction mechanism.[17–19] Titanium(IV) compounds, especially titanium alkoxides, are often employed as esterifica-

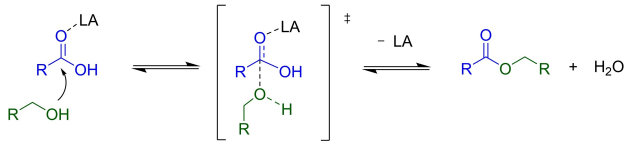

Scheme 1. Schematic representation for Lewis acid (LA) catalyzed esterification.

[a] L. A. Wolzak, Prof. M. Tromp, Dr. T. J. Korstanje
Sustainable Materials Characterization
van 't Hoff Institute for Molecular Sciences (HIMS)
University of Amsterdam
Science Park 904
1098 XH Amsterdam (The Netherlands)
E-mail: t.j.korstanje@uva.nl
moniek.tromp@rug.nl
[b] Dr. J. I. van der Vlugt, Prof. J. N. H. Reek
Bio-inspired, Homogeneous and Supramolecular Catalysis
van 't Hoff Institute for Molecular Sciences (HIMS)
University of Amsterdam
Science Park 904
1098 XH Amsterdam (The Netherlands)
E-mail: j.n.h.reek@uva.nl
[c] Dr. J. I. van der Vlugt
Bioinspired Coordination Chemistry & Catalysis
Institute of Chemistry
Carl von Ossietzky University Oldenburg
Carl-von-Ossietzky-Strasse 9–11
26129 Oldenburg (Germany)
[d] Dr. K. J. van den Berg
Akzo Nobel Car Refinishes BV
Rijksstraatweg 31
2171 AJ Sassenheim (The Netherlands)
[e] Prof. M. Tromp
Faculty of Science and Engineering
Materials Chemistry – Zernike Institute for Advanced Materials
University of Groningen
Nijenborgh 4
9747 AG Groningen (The Netherlands)

Supporting information for this article is available on the WWW under https://doi.org/10.1002/cctc.202000931

tion catalyst due to their inherent Lewis acidity and non-toxic nature.[20–23] Mechanistic insight into the role of these titanium derivatives is, however, hampered by the rapid uncontrolled exchange reactions with carboxylic acids, alcohols and esters (Figure 1).[24,25] In addition, facile hydrolysis leads to very complex reaction mixtures consisting of titaniumdioxide, oxo-alkoxides and oligomeric structures.[26–28] Here, we report a mechanistic investigation on the use of titanium aminotriphenolate complexes showing the amphoteric nature of the catalyst. Both the Lewis acidity and Brønsted basicity are important for the overall performance in esterification reactions. The catalysts based on the tetradentate aminotriphenolate ligands are robust, display remarkable stability to hydrolysis and are stable under acidic conditions.[29–32] This can be of importance for the application of these complexes, and the stability also allows the isolation of relevant reaction intermediates. The steric and electronic properties of the tetradentate aminotriphenolate ligand can be modified, making it a perfect platform for optimization of catalyst properties and a detailed mechanistic study (Figure 1).[33]

Results and Discussion

Aminotriphenols **1**–**5** (Scheme 2) are readily available via electrophilic aromatic substitution of the corresponding phenol with hexamethylenetetramine or reductive amination of the appropriate salicylic aldehydes.[34–36] The reaction of $Ti(O^iPr)_4$ with one equiv. of **1**–**5** yielded the mononuclear, C_3-symmetric complexes **6**–**10**.[37] Ligand exchange of the apical isopropoxide group is facile under acidic conditions.[32] Reaction of complex **6** with 20 equivalents of acetic acid resulted in complex **11**, which was isolated as an orange powder. ^{1}H NMR analysis revealed a sharp singlet corresponding to the six methylene hydrogens in the ligand framework, a broad singlet corresponding to six hydrogens of two acetate fragments and also a strongly deshielded signal at 14.5 ppm, integrating for one hydrogen (Figure S7). This indicates that besides apical exchange of the isopropoxide for an acetate ligand, an intact acetic acid molecule has also entered the coordination sphere of Ti^{IV}, resulting in an overall octahedral coordination. Upon addition of D_2O to species **11**, the strongly downfield signal disappeared, demonstrating facile exchange of the acidic hydrogen of acetic acid (Figure S8). The singlet for the methylene hydrogens is remarkable, as it reveals that the barrier for inversion of the rotor-shaped ligand is significantly lower than in complex **6**.[37] In addition, a variable temperature ^{1}H NMR experiment further supported that both an acetate and an acetic acid group are coordinated to the titanium center: Six doublets corresponding to three different methylene groups are observed at −65 °C, indicating loss of C_3 symmetry of this complex (Figure S11). Suitable crystals for single crystal X-ray diffraction were obtained via slow evaporation of a benzene solution of complex **11**. The molecular structure (Figure 2) displays a slightly distorted octahedral complex with an O1–Ti–O2 angle of 98.13(5)°. The difference in C–O bond lengths of the two carboxylate moieties indicates coordination of both an acetate and an acetic acid group to titanium, with the proton (H1) sandwiched between both groups.

To demonstrate that the apical exchange of the isopropyl group is also possible for sterically less encumbered ligands, the unsubstituted complex **10** was treated with an excess of acetic acid. Attempts to isolate the newly formed complex proved to be cumbersome, but *in situ* formation of the acetic acid/acetate complex **12** was demonstrated by ^{1}H NMR spectroscopy (Figure S12).

We studied the catalytic activity of complexes **6**–**10** (1 mol%) in a model esterification reaction between benzoic acid and heptanol in a 1:10 ratio (Table 1). An excess of the alcohol was used in order to drive the reaction to completion without the need for dehydrating agents or azeotropic distillation, and a reaction time of 6 h was used to enable the observation of distinct differences in catalytic activity. The uncatalyzed reaction hardly provided any heptylbenzoate (entry 1), while the presence of catalytic amounts of complexes **6**–**8** gave a moderate increase in the efficiency of the reaction

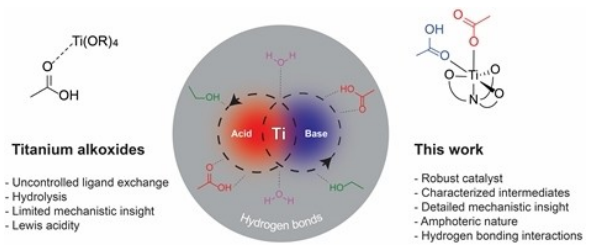

Figure 1. Comparison between titanium(IV) alkoxides and the titanium aminotriphenolate catalyst studied here.

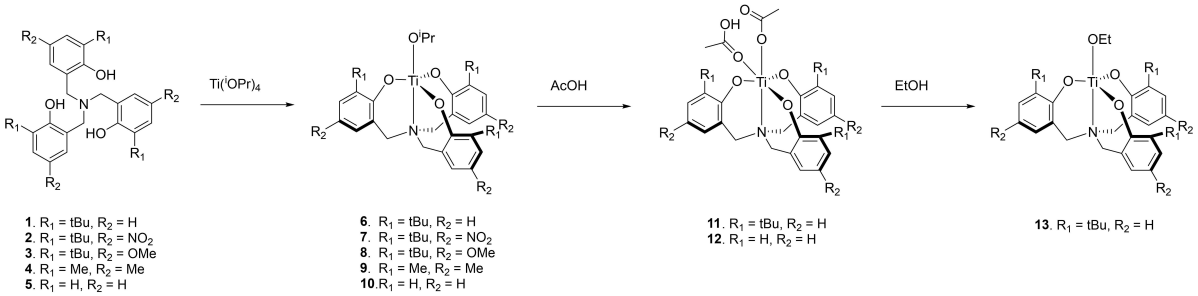

Scheme 2. Aminotriphenol ligands **1**–**5** and corresponding titanium complexes **6**–**13**.

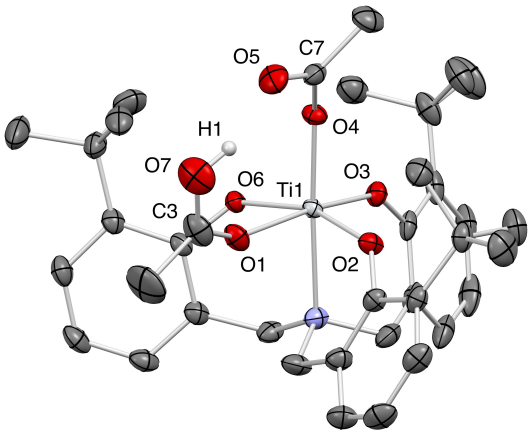

Figure 2. ORTEP view of solid state structure of complex **11**. Ellipsoids are given at 50% probability level. H atoms, except for H1 in between O7 and O5, and disorder in C3 and O7 are omitted for clarity. Selected bond distances (Å): Ti1–O1 = 1.864(1), Ti1–O2 = 1.823(1), Ti1–O3 = 1.878(1), Ti1–O4 = 1.947(1), Ti1–O6 = 2.120(1), Ti1–N1 = 2.239(1), C3–O6 = 1.24(1), C3–O7 = 1.29(2), C1–O4 = 1.287(2), C1–O5 = 1.237(2). Selected angles (°): N1–Ti1–O4 = 176.07(5), O4–Ti1–O6 = 92.33(5), O1–Ti1–O2 = 98.13(5). Colors correspond to titanium (light gray), oxygen (red), nitrogen (purple), and carbon (gray).

Table 1. Catalyst screening in model esterification reaction.

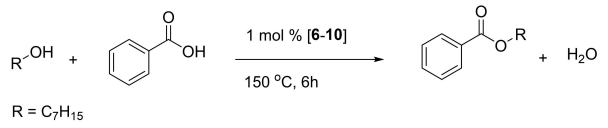

R = C_7H_{15}

Entry[a]	Complex	Conv. [%] Benzoic acid	Yield [%] Heptyl benzoate
1	no cat.	10	6
2	**6**	31	26
3	**7**	40	36
4	**8**	19	19
5	**9**	48	48
6	**10**	62	62
7	$Ti(O^iPr)_4$	79	79

[a] All reactions were performed with benzoic acid (5 mmol), heptanol (50 mmol), and Ti catalyst (1 mol%, 0.05 mmol), at 150 °C for 6 h. Yield and conversion were determined by GC analysis with pentadecane as internal standard.

(entries 2–4). The reaction with the sterically less hindered complexes **9**–**10** resulted in a further increase in yield (48% and 62%, entries 5 and 6), although they could not match the activity of $Ti(O^iPr)_4$ (79% yield, entry 7). The trend in activity for catalysts **6**–**8** (**8** > **6** > **7**), related to the electronic properties of the phenoxy ligands (OMe > H > NO_2), suggesting that a more Lewis acidic titanium center leads to higher activity. In addition, the steric bulk in the *ortho*-position of the phenol motif of complexes **6** and **9** clearly impedes activity in catalysis (entries 2 and 5). In separate experiments complex **10** and $Ti(O^iPr)_4$ provided full conversion of benzoic acid after 24 h reaction time (> 99% yield of heptyl benzoate, Figure S1). Furthermore, the addition of molecular sieves as dehydrating agent had a marginal influence on the rate of formation of heptylbenzoate (Figure S1). To investigate the reaction mechanism underlying the titanium aminotriphenolate-catalyzed esterification, initial kinetic and stoichiometric experiments were performed. For complex **10** an order in catalyst of 0.80 was found in the concentration range 1.56 to 9.33 mM (0.25 to 1.5 mol%) (Figure S2, Table S1), which lends support to a mononuclear mechanism.[38] The activation energy was experimentally determined via an Arrhenius plot of the different rates of the reaction between 150–180 °C (Figure S3, Table S2). We found an energy of 20.1 kcal mol^{-1}, which is in good agreement with other titanium based esterification catalysts.[25]

In order to establish the resting state during catalysis, an aliquot was taken from the model esterification reaction catalyzed by complex **6** after 30 minutes reaction time, and studied with mass spectrometry. The two observed species have an experimental mass of 669.3291 *m/z* and 663.4111 *m/z* which correlates to complexes where the apical isopropoxide group is exchanged for a heptoxy or a benzoate group (Figure S22). To further deduce the exact structure of the resting state, complex **6** was treated with 10 equiv. of acetic acid and 100 equiv. of ethanol in toluene at 110 °C. After 24 h, at which point the reaction had not yet reached completion, the mixture was evaporated and complex **11** was isolated with only minor impurities, suggesting that in the resting state both a carboxylate and a carboxylic acid are coordinated to titanium.[39] To demonstrate the facile formation of the alkoxy-substituted complex, complex **11** was dissolved in an excess of dry ethanol and stirred for 15 min. at RT. After evaporation of the solvent the new complex **13** was isolated (Scheme 2), bearing an ethoxy group in the apical position, as determined by NMR spectroscopy and mass spectrometry. Given these results, we conclude that complex **11** is the resting state during catalysis, while complex **13** is the end-of-catalysis state when an excess of alcohol is used, and possibly also an off-cycle complex.

The reaction mechanism for the most active titanium aminotriphenolate complex **10** was further examined with DFT-D3 calculations at the BP86/TZ2P level of theory (Figure 3, see Supporting Information for other, energetically less favorable calculated reaction pathways (Figure S24)).[40,41] The reaction starts with the acetic acid/acetate complex **A**, which is an analogue of the well characterized complex **11**, followed by transition state $\mathbf{TS_{AB}}$, involving a rotation of the apical acetic acid. Intermediate **B** is significantly higher in energy than complex **A** ($\Delta G = 7.6$ kcal mol^{-1}), due to the loss of the favorable hydrogen bonding interaction between the acetic acid and the acetate group. Nucleophilic attack of the alcohol is facile with a $\Delta\Delta G^{\ddagger}$ of 6.9 kcal mol^{-1} for $\mathbf{TS_{CD}}$. This step is favorable because the alcoholic hydrogen is hydrogen bonded to the acetate group that can also accept the proton and thus acts as an internal base. The combined action of a Brønsted basic acetate group and a Lewis acidic titanium center, results in overall amphoteric character for this catalyst. The beneficial effect of using an amphoteric catalyst for esterification reactions has already been observed for metal hydroxides and alkoxides in the 1960s,[42] but is rarely mentioned in more recent studies. The next transition state, $\mathbf{TS_{DE}}$, involves a rotation which requires the cleavage of two hydrogen bonds, in order to pre-

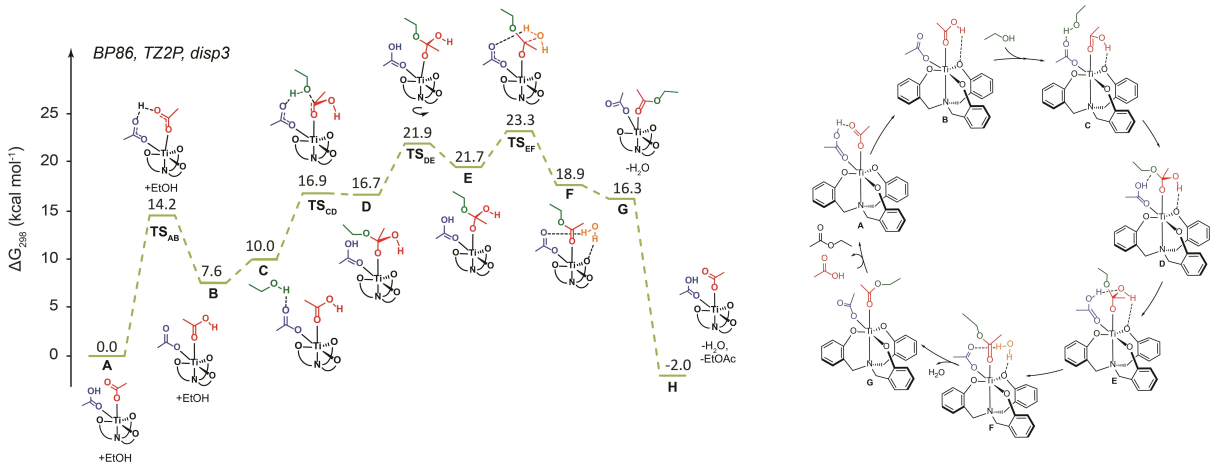

Figure 3. Proposed reaction pathway for the esterification reaction catalyzed by complex **10** (in the catalytic cycle hydrogen bonds are indicated with black dashed lines).

organize intermediate **E** for water formation. The third transition state, $\mathbf{TS_{EF}}$, concerns the actual cleavage of the carbon-hydroxyl oxygen bond in structure **E** in order to form the ester. Consecutive loss of water and the ester product results in an overall slightly exergonic process ($\Delta G = -2.0$ kcal mol^{-1}). The total energy profile shows that two transitions states ($\mathbf{TS_{DE}}$ and $\mathbf{TS_{EF}}$) are close in free energy (1.3 kcal mol^{-1}), showing that both these transitions state can be the rate determining transition state.

The optimized structures for the transition states $\mathbf{TS_{DE}}$ and $\mathbf{TS_{EF}}$ reveal the presence of hydrogen bonding interactions (Figure 4). During $\mathbf{TS_{DE}}$, hydrogen bonds are formed between H_A and O_B of the ligand framework as well as between the acetic acid hydrogen (H_B) and O_A. These interactions pre-organize the complex for water formation (intermediate **E**) and are thus necessary to enhance the next step in the reaction, where water is expelled. Hydrogen bonding interactions between both water hydrogens (H_A and H_B) and the ligand oxygen (O_B) and the substrate oxygen (O_A) respectively, remain in $\mathbf{TS_{EF}}$, showing that these contribute to a lower energy of this rate determining transition state, thus enhancing the overall reaction rate.

Additional DFT calculations were performed to evaluate the catalytic activity of Ti complexes based on the C_3-symmetric tetradentate ligand with different *para*-substituents on the aromatic rings (Table 2). These calculations show that for the transition states $\mathbf{TS_{CD}}$, $\mathbf{TS_{DE}}$ and $\mathbf{TS_{EF}}$ the relative barrier, $\Delta\Delta G^{\ddagger}$ (the free energy difference between the transition state and its preceding intermediate), is indeed lowered by an electron-withdrawing nitro-substituent (entry 1), which leads to a more Lewis acidic metal center. However, the effect of a *para*-substituent on the overall activation energy of the reaction is small, with only 0.6 kcal mol^{-1} difference between the methoxy- or nitro-substituted versions and the unsubstituted ligand, thus showing that here the Lewis acidity of the metal center is only a minor factor to modulate the overall activation energy and reaction rate.

Based on these kinetic experiments and DFT calculations, we propose a catalytic cycle as depicted in Figure 3. In all geometries, including transition states, hydrogen bonding interactions are present between the ligand, the acetate/acetic acid group and the alcohol. Nucleophilic attack by the alcohol has a moderate energy barrier due to favorable preorganization of both the alcohol and the titanium-bound acetic acid via hydrogen bonding interactions with the acetate group and an oxygen of the ligand framework. As a result, proton transfer from the alcohol to the acetate group, which acts as a proton reservoir for water formation, is facile. $\mathbf{TS_{DE}}$ is a rotation, which requires the breakage of a hydrogen bond, in order to have the adequate geometry for water formation. The subsequent carbon-oxygen bond breaking, $\mathbf{TS_{EF}}$, therefore has a notably low

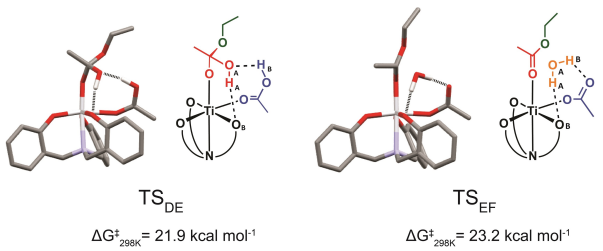

Figure 4. Calculated transition states $\mathbf{TS_{DE}}$ and $\mathbf{TS_{EF}}$ (optimized with DFT-D3 at the BP86/def-TZ2P level of theory) and ChemDraw representations thereof. All hydrogen atoms have been omitted for clarity (except hydrogens A and B involved in hydrogen bonds, indicated with black dashed lines).

Table 2. Influence of the *para*-substituent of the ligand on the relative barrier and the overall barrier of transition states $\mathbf{TS_{CD}}$, $\mathbf{TS_{DE}}$ and $\mathbf{TS_{EF}}$.

		TS_{CD}		TS_{DE}		TS_{EF}	
Entry[a]	Para-substituent	$\Delta\Delta G^{\ddagger}$	$\Delta G^{\ddagger}$	$\Delta\Delta G^{\ddagger}$	$\Delta G^{\ddagger}$	$\Delta\Delta G^{\ddagger}$	$\Delta G^{\ddagger}$
1	$-NO_2$	6.1	16.4	5.1	21.2	3.5	22.6
2	–H	6.8	16.8	5.3	21.9	3.7	23.2
3	–OMe	7.5	16.1	6.1	22.6	4.0	22.6

[a] Values are given in kcal mol^{-1}.

barrier for a bond-breaking step. Overall, this mechanism shows that there are three essential prerequisites for an active catalyst: Lewis acidity of the Ti metal, favorable hydrogen bonding interactions between both reactants and the ligand, and a Brønsted basic group to facilitate proton transfer. This is in strong contrast with the common assumption that the Lewis acidity of the metal is the sole crucial (rate determining) factor for catalytic activity. The generality of our findings is demonstrated by the fate of many esterification catalysts under reaction conditions. The acidic reaction medium results in ligand exchange reactions, leading to the *in situ* formation of amphoteric metal carboxylates,[24] which could well have a similar mode of operation as the titanium aminotriphenolates presented in this study.

Conclusion

In summary, we have shown that the amphoteric nature of Ti-aminotriphenolate complexes, combining a Lewis acidic metal center with a Brønsted basic ligand site, in combination with preorganization via hydrogen bonding interactions, is essential for the catalytic activity of titanium aminotriphenolate complexes in the esterification reaction. Experimental and computational findings demonstrate that Lewis acidity is not the only key factor for catalytic activity, contrary to what often is assumed in literature. DFT calculations support favorable preorganization via hydrogen bonding interactions with the ligand and elucidate the role of the additional acetate group as internal base. This acetate group enhances the nucleophilicity of the alcohol and subsequently stores the proton of the alcohol, which later on in the reaction is expelled in the form of water. We believe that these insights do not only apply to this particular class of titanium complexes, but are also important for other esterification catalysts, including often-used titanium alkoxides, and as such can help the rational design of new catalysts for esterification reactions.

Experimental Section

General Experimental Details

Dichloromethane and acetonitrile were distilled from CaH_2, *n*-pentane and Et_2O from sodium/benzophenone and toluene from sodium under argon atmosphere. Ethanol was degassed and dried over 3 Å molecular sieves. All other chemicals were obtained from Merck or Fluorochem and were used without further purification. All air-sensitive materials were manipulated using standard Schlenk techniques or by the use of an argon-filled glovebox (MBraun Unilab). The NMR solvents CD_2Cl_2, toluene-d_8 and C_6D_6 were dried over molecular sieves and degassed via three cycles of freeze-pump-thaw. ^1H and ^{13}C NMR spectra were recorded on a 300 or 400 MHz Bruker AVANCE spectrometer. Spectra were referenced against residual solvent signal. FD-MS spectra were collected on an AccuTOF GC v 4 g, JMS-T100GCV Mass spectrometer (JEOL, Japan) equipped with a Carbotec emitter. A typical current rate of 51.2 mA min^{-1} over 1.2 min and a flashing current 40 mA on every spectra of 30 ms was used. High resolution ESI-MS spectra were recorded on a JEOL AccuTOF LC-Plus JMS-T100LP spectrometer in CH_3CN. IR spectra were recorded on a Bruker Alpha FTIR machine. GC analysis for heptylbenzoate and benzoic acid was performed on a Thermo Scientific Trace GC Ultra equipped with a Restek Stabilwax-DA column (30 m × 0.25 mm × 0.25 μm). Temperature program: initial temperature 50 °C, heat to 200 °C with 20 °C min^{-1}, hold for 10 min, heat to 250 °C with 50 °C min^{-1}, hold for 3 minutes. Inlet temperature 250 °C, split ratio of 30, 1.0 mL min^{-1} helium flow, FID temperature 250 °C. Esterification reactions were performed in a Radley Discoveries 12 plus reaction station allowing a maximum of 12 simultaneous reactions under a nitrogen atmosphere.

Single crystal X-ray diffraction

X-ray Crystal Structure Determination of complex **11**: X-ray intensities were measured on a Bruker D8 Quest Eco diffractometer equipped with a Triumph monochromator (I = 0.71073 Å) and a CMOS Photon 100 detector at a temperature of 150(2) K. Intensity data were integrated with the Bruker APEX3 software.[43] Absorption correction and scaling was performed with SADABS.[44] The structures were solved using intrinsic phasing with the program SHELXT.[45] Least-squares refinement was performed with SHELXL-2014[46] against F2 of all reflections. Non-hydrogen atoms were refined with anisotropic displacement parameters. The H atoms were placed at calculated positions using the instructions AFIX 13, AFIX 43 or AFIX 137 with isotropic displacement parameters having values 1.2 or 1.5 times Ueq of the attached C atoms. CCDC 1941519 contain the supplementary crystallographic data for this paper. These data can be obtained free of charge from The Cambridge Crystallographic Data Centre via www.ccdc.cam.ac.uk/data_request/cif.

Computational details

Geometry optimizations were carried out with the Amsterdam Density Functional (ADF) program package using version 2017.201.[40,41] We used the BP86 functional in combination with the TZ2P basis set and a large frozen core.[47–49] Grimme's dispersion corrections (version 3, disp3) were used to include Van der Waals interactions.[50] All minima (no imaginary frequencies) and transition states (one imaginary frequency) were characterized by calculating the Hessian matrix. ZPE and gas-phase thermal corrections (enthalpy, 298 K) from these analyses were calculated.

Synthesis and catalysis

The triphenolamines **1**–**5** and titanium complexes **6**–**10** were synthesized via literature procedures.[34–37]

Complex 7

Under nitrogen atmosphere ligand **2** (100 mg, 0.16 mmol) was dissolved in 10 mL dry Et_2O. This solution was slowly added to $Ti(O^iPr)_4$ (46 μL, 0.16 mmol) in 5 mL dry Et_2O. The reaction mixture immediately changed to orange and over a period of 12 h a pale yellow precipitate formed. After filtration the solid material was dissolved in a minimum amount of DCM and precipitated with Et_2O (15 mL). Subsequent filtration afforded complex **7** (76 mg, 64 %). ^1H NMR (300 MHz, CD_2Cl_2): δ 8.19 (d, J = 2.8 Hz, 3H, $\underline{H}_{Ar}$), 8.01 (d, J = 2.8 Hz, 3H, $\underline{H}_{Ar}$), 3.58 (br s, 6H, $NC\underline{H}_2$), 1.58 (d, J = 6.2 Hz, 6H, $OCHC\underline{H}_3$), 1.51 (s, 27H, tBu), the $OC\underline{H}(CH_3)_2$ proton overlaps with the solvent peak (δ 5.32). ^1H NMR (300 MHz, C_6D_6): δ 8.32 (d, J = 2.8 Hz, 3H, $\underline{H}_{Ar}$), 7.77 (d, J = 2.7 Hz, 3H, $\underline{H}_{Ar}$), 5.18 (h, J = 6.0 Hz, 1H, $OC\underline{H}(CH_3)_2$), 2.88 (br s, 3H, $NC\underline{H}_2$), 2.19 (br s, 3H, $NC\underline{H}_2$), 1.47 (d, J = 6.1 Hz, 6H, $OCHC\underline{H}_3$), 1.35 (s, 27H, tBu). ^{13}C NMR (100 MHz, CD_2Cl_2): δ 167.20

($\underline{C}_{Ar}$), 141.22 ($\underline{C}_{Ar}$), 138.32 ($\underline{C}_{Ar}$), 125.33 ($\underline{C}_{Ar}$), 124.05 ($\underline{C}H_{Ar}$), 123.62 ($\underline{C}H_{Ar}$), 84.03 ($\underline{C}H(CH_3)_2$), 58.13 ($N\underline{C}H_2$), 35.61 ($\underline{C}(CH_3)_3$), 29.34 (C($\underline{C}H_3)_3$), 26.40 (OCH($\underline{C}H_3)_2$). FD-MS (*m/z, pos*): Calculated for $[C_{36}H_{46}N_4O_{10}Ti]$ 742.2697; found 742.2679 $[M]^+$.

Complex 11

Under nitrogen atmosphere Complex **6** (100 mg, 0.165 mmol) was dissolved in 5 mL dry toluene and 20 equivalents of acetic acid (188 μL, 3.29 mmol) were added dropwise to give an orange reaction mixture. After stirring at room temperature for 10 min the solvent was removed in vacuo. The remaining orange powder was triturated three times with 10 mL dry acetonitrile and dried under vacuum. Yield 102 mg (93%). ^{1}H NMR (400 MHz, CD_2Cl_2): δ 14.51 (s, 1H, O–$\underline{H}$–O), 7.21 (d, J = 6.2 Hz, 3H, $\underline{H}_{Ar}$), 7.02 (d, J = 7.4 Hz, 3H, $\underline{H}_{Ar}$), 6.77 (t, J = 7.6 Hz, 3H, $\underline{H}_{Ar}$), 3.74 (s, 3H, $NC\underline{H}_2$), 1.85 (br s, 6H, $C\underline{H}_3$), 1.39 (s, 27H, $C(C\underline{H}_3)_3$). Addition of D_2O resulted in the disappearance of the singlet at δ 14.51 and a new singlet at δ 4.76 (HDO). ^{13}C NMR (125 MHz, CD_2Cl_2): δ 178.28 (br s, $OO\underline{C}CH_3$), 161.66 ($\underline{C}_{Ar}$), 136.69 ($\underline{C}_{Ar}$), 127.83 ($\underline{C}H_{Ar}$), 126.88 ($\underline{C}H_{Ar}$), 125.55 ($\underline{C}_{Ar}$), 120.33 ($\underline{C}H_{Ar}$), 60.89 ($N\underline{C}H_2$), 35.01 ($\underline{C}(CH_3)_3$), 29.87 ($C(\underline{C}H_3)_3$). The methyl carbons of the acetate and acetic acid group were not observed due to their fluxional behavior. FD-MS (*m/z, pos*): Calculated for $[C_{36}H_{48}NO_4Ti]$ 607.2777; found 607.2948 $[M-CH_3COOH]^+$. ESI-MS (*m/z, pos*): Calculated for $[C_{33}H_{42}NO_3Ti]$ 548.26475; found 548.26665 $[M-CH_3COO-CH_3COOH]^+$. IR-ATR (cm^{-1}): 1658 (s, $\nu_{as\ COO}$). Crystals suitable for X-ray analysis were grown via slow evaporation of a concentrated benzene solution.

$C_{37}H_{49}NO_7Ti$, Fw = 667.67, plate, 0.560 × 0.537 × 0.267 mm, monoclinic, P21/c (No: 14)), a = 17.7368(10), b = 11.9329(6), c = 18.0144(10) Å, β = 110.227(2)°, V = 3577.6(3) Å^3, Z = 4, Dx = 1.240 g/cm^3, m = 0.287 mm^{-1}. 132094 Reflections were measured up to a resolution of (sin q/l)max = 0.77 Å^{-1}. 8199 Reflections were unique (Rint = 0.0399), of which 7049 were observed [I > 2 s(I)]. 452 Parameters were refined with 105 restraints. R1/wR2 [I > 2 s(I)]: 0.0382/0.0922. R1/wR2 [all refl.]: 0.0482/0.0989. S = 1.076. Residual electron density between −0.402 and 0.318 e/Å^3. CCDC 1941519.

Complex 12

Complex **10** (5 mg, 0.01 mmol) was reacted with acetic acid (10 μL, 0.18 mmol) in dry C_6D_6 in an NMR tube under nitrogen atmosphere. ^{1}H NMR (400 MHz, C_6D_6): δ 7.12–6.55 (m, 12H, $\underline{H}_{Ar}$), 3.74 (br s, 1H, free $C\underline{H}OH(CH_3)_2$), 3.38 (s, 6H, $NC\underline{H}_2$), 0.99 (d, J = 5.8, 6H, free (CHOH($C\underline{H}_3)_2$). The methyl groups of the coordinated acetic acid and acetate group are not observed due to exchange with free acetic acid.

Complex 13

Complex **11** (34 mg, 0.05 mmol) was dissolved in 2 mL dry EtOH under nitrogen atmosphere to give a yellow suspension after 30 minutes of stirring at room temperature. Removal of ethanol and residual acetic acid in vacuo resulted in the isolation of complex **13** as a pale yellow powder (28 mg, 92%). ^{1}H NMR (400 MHz, C_6D_6): δ 7.38 (d, J = 7.7 Hz, 3H, $\underline{H}_{Ar}$), 6.92 (d, J = 7.5 Hz, 3H, $\underline{H}_{Ar}$), 6.85 (d, J = 7.3 Hz, 3H, $\underline{H}_{Ar}$), 5.20 (q, J = 7.0 Hz, 2H, $OC\underline{H}_2CH_3$), 3.98 (br s, 3H, $NC\underline{H}_2$), 2.57 (br s, 3H, $NC\underline{H}_2$), 1.74 (t, J = 6.9 Hz, 3H, $OCH_2C\underline{H}_3$), 1.72 (s, 27H, $C(C\underline{H}_3)_3$). ^{13}C NMR (100 MHz, C_6D_6): δ 167.76 ($\underline{C}_{Ar}$), 136.16 ($\underline{C}_{Ar}$), 126.26 ($\underline{C}H_{Ar}$), 125.06 ($\underline{C}_{Ar}$), 120.24 ($\underline{C}H_{Ar}$), 73.14 ($O\underline{C}H_2CH_3$), 58.23 ($\underline{C}$), 34.71 ($\underline{C}$), 29.44 ($C(\underline{C}H_3)_3$), 19.46 ($OCH_2\underline{C}H_3$). One of the aromatic carbons, $\underline{C}H_{Ar}$, overlaps with the C_6D_6 signal at δ 128.06, see cross peak in HSQC (6.85; 128.06). FD-MS (*m/z, pos*): Calculated for $[C_{35}H_{47}NO_4Ti]$ 593.2988; found 593.2982.

Reaction of complex 6 with acetic acid and ethanol

To examine the formation of complex 15 during catalysis, a solution of complex **6** (30 mg, 0.05 mmol) in 5 mL dry toluene was reacted with 20 equivalents acetic acid (57 μL, 0.97 mmol) and ~200 equivalents of ethanol (575 μL, 9.86 mmol). The reaction mixture was brought to reflux and stirred for 24 h. An aliquot was taken and ethyl acetate was detected by GC analysis. About 2.5 mL of the reaction mixture was evaporated to dryness which resulted in the isolation of complex **11** with minor impurities (~10 mg, 61%). ^{1}H NMR (300 MHz, CD_2Cl_2): δ 7.21 (d, J = 6.2 Hz, 3H, $\underline{H}_{Ar}$), 7.02 (d, J = 7.4 Hz, 3H, $\underline{H}_{Ar}$), 6.77 (t, J = 7.6 Hz, 3H, $\underline{H}_{Ar}$), 3.74 (s, 6H, $NC\underline{H}_2$), 1.83 (br s, 6H, $C\underline{H}_3$), 1.39 (s, 27H, $C(C\underline{H}_3)_3$). The COO$\underline{H}$ proton at δ 14.51 was not observed.

Procedure for esterification of benzoic acid and heptanol

In a carousel reaction station under a nitrogen atmosphere benzoic acid (610.6 mg, 5 mmol) was dissolved in heptanol (7.14 mL, 50 mmol). The catalyst (1 mol%) was added as a powder, except from Ti($O^iPr)_4$, and pentadecane (0.41 mL, 1.5 mmol) as internal standard. The reaction mixture was heated up to 150 °C. After 6 h the conversion and yield were determined with GC analysis via the integration of the peak area of benzoic acid and heptylbenzoate. In order to achieve full conversion the reaction time was extended to 24 h for a selection of catalysts. The effect of a dehydrating agent was studied via the addition of 1 g of activated powder molecular sieves (4 Å).

Acknowledgements

This work is part of the Advanced Research Center for Chemical Building Blocks, ARC CBBC, which is co-founded and co-financed by the Netherlands Organisation for Scientific Research (NWO, contract 736.000.000) and the Netherlands Ministry of Economic Affairs and Climate. In addition, the authors thank NWO for funding VENI grant 722.016.012 (to T.J.K.). The authors thank Jan-Meine Ernsting, Dr. Andreas Ehlers and Ed Zuidinga for NMR spectroscopy and mass spectrometry support, Prof. Dr. Bas de Bruin for aid and suggestions in the performed DFT calculations, Dr. Maxime Siegler for his tips and tricks for refining the X-ray crystal structure and Bastiaan Beerman and Renske Grupstra for help during the laboratory experiments.

Conflict of Interest

The authors declare no conflict of interest.

Keywords: Homogeneous Catalysis · Esterification · Titanium, Amphoteric · Hydrogen bonding interactions

[1] J. Otera, J. Nishikido, *Esterification. Methods, Reactions, and Applications*, Wiley-VCH Verlag GmbH & Co., Weinheim, **2010**.
[2] A. Fischer, E. Speier, *Chem. Ber.* **1895**, *28*, 3252–3258.
[3] J. Clayden, N. Greeves, S. Warren, *Organic Chemistry*, Oxford University Press, Oxford, **2012**.
[4] Y. Román-Leshkov, M. E. Davis, *ACS Catal.* **2011**, *1*, 1566–1580.

[5] J. J. Li, *Fischer-Speier Esterification. In: Name Reactions*, Springer, Berlin, Heidelberg, **2002**.
[6] G. Bartoli, J. Boeglin, M. Bosco, M. Locatelli, M. Massaccesi, P. Melchiorre, L. Sambri, *Adv. Synth. Catal.* **2005**, *347*, 33–38.
[7] T. Kawabata, T. Mizugaki, K. Ebitani, K. Kaneda, *Tetrahedron Lett.* **2003**, *44*, 137–140.
[8] H. E. Hoydonckx, D. E. De Vos, S. a Chavan, P. A. Jacobs, *Top. Catal.* **2004**, *27*, 83–96.
[9] A. B. Ferreira, A. Lemos Cardoso, M. J. da Silva, *ISRN Renewable Energy* **2012**, *2012*, 1–13.
[10] J. Bahamonde Santos, A. Martinez, M. Mira, *Chem. Eng. Technol.* **1996**, *19*, 538–542.
[11] K. Ishihara, M. Nakayama, S. Ohara, H. Yamamoto, *Tetrahedron* **2002**, *58*, 8179–8188.
[12] M. Nakayama, A. Sato, K. Ishihara, H. Yamamoto, *Adv. Synth. Catal.* **2004**, *346*, 1275–1279.
[13] D. Dupont, S. Arnout, P. T. Jones, K. Binnemans, *J. Sustain. Metall.* **2016**, *2*, 79–103.
[14] K. Ishihara, S. Ohara, H. Yamamoto, *Science* **2000**, *290*, 1140–1142.
[15] M. R. Meneghetti, S. M. P. Meneghetti, *Catal. Sci. Technol.* **2015**, *5*, 765–771.
[16] K. Manabe, S. Kobayashi, *Adv. Synth. Catal.* **2002**, *344*, 270–273.
[17] F. Pilati, P. Manaresi, B. Fortunato, A. Munari, V. Passalacqua, *Polymer* **1981**, *22*, 1566–1570.
[18] F. Pilati, P. Manaresi, B. Fortunato, A. Munari, P. Monari, *Polymer* **1983**, *24*, 1479–1483.
[19] W. Tian, Z. Zeng, W. Xue, Y. Li, T. Zhang, *Chin. J. Chem. Eng.* **2010**, *18*, 391–396.
[20] L. Chen, J. Xu, W. Xue, Z. Zeng, *Korean J. Chem. Eng.* **2018**, *35*, 82–88.
[21] R. Wiegner, J. Voerckel, V. Runkel, D. Eckert, *Titanium-Based Catalyst Showing Excellent Activity and Selectivity in Polycondensation Reactions*, **2012**, US2012/0316316.
[22] F. Ahmadnian, F. Velasquez, K. H. Reichert, *Macromol. React. Eng.* **2008**, *2*, 513–521.
[23] Y. Yang, S. Yoon, Y. Hwang, B. Song, *Bull. Korean Chem. Soc.* **2012**, *33*, 3445–3447.
[24] E. Leverd, F. Fradet, A. Maréchal, *Eur. Polym. J.* **1987**, *23*, 695–698.
[25] E. Fradet, A. Maréchal, in *Adv. Polym. Sci.*, Springer Berlin Heidelberg, **1982**.
[26] K. Pang, R. Kotek, A. Tonelli, *Prog. Polym. Sci.* **2006**, *31*, 1009–1037.
[27] M. Bonchio, G. Licini, G. Modena, O. Bortolini, S. Moro, W. A. Nugent, *J. Am. Chem. Soc.* **1999**, *121*, 6258–6268.
[28] S. Doeuff, M. Henry, C. Sanchez, J. Livage, *J. Non-Cryst. Solids* **1987**, *89*, 206–216.
[29] S. Gendler, S. Segal, I. Goldberg, Z. Goldschmidt, M. Kol, *Inorg. Chem.* **2006**, *45*, 4783–4790.
[30] C. Zonta, E. Cazzola, M. Mba, G. Licini, *Adv. Synth. Catal.* **2008**, *350*, 2503–2506.
[31] S. D. Bull, M. G. Davidson, C. L. Doherty, A. L. Johnson, M. F. Mahon, *Chem. Commun.* **2003**, 1750–1751.
[32] V. Ugrinova, G. A. Ellis, S. N. Brown, *Chem. Commun.* **2004**, 468–469.
[33] G. Licini, M. Mba, C. Zonta, *Dalton Trans.* **2009**, 5265–5277.
[34] L. J. Prins, M. M. Blázquez, A. Kolarović, G. Licini, *Tetrahedron Lett.* **2006**, *47*, 2735–2738.
[35] D. Lionetti, A. J. Medvecz, V. Ugrinova, M. Quiroz-Guzman, B. C. Noll, S. N. Brown, *Inorg. Chem.* **2010**, *49*, 4687–4697.
[36] P. Zardi, K. Wurst, G. Licini, C. Zonta, *J. Am. Chem. Soc.* **2017**, *139*, 15616–15619.
[37] M. Kol, M. Shamis, I. Goldberg, Z. Goldschmidt, S. Alfi, E. Hayut-Salant, *Inorg. Chem. Commun.* **2001**, *4*, 177–179.
[38] Given the catalyst order of 0.8, we believe that the system is primarily catalyzed by mononuclear titanium complexes, although a minor contribution of dimeric species that dissociate during the rate-determining step, lowering the reaction order, cannot be excluded. In addition, the order in carboxylic acid and alcohol are outside the scope of this research, since the very high concentrations of both reactants makes order determination cumbersome. Moreover, a considerable Brønsted acid-catalyzed (background) reaction also takes place, making both reactant orders non-informative for the titanium-catalyzed reaction, see reference.[24].
[39] For all octahedral complexes with a carboxylate and a carboxylic acid group coordinated to titanium, the carboxylic acid group was not observed with mass spectrometry.
[40] G. te Velde, F. M. Bickelhaupt, E. J. Baerends, C. Fonseca Guerra, S. J. A. van Gisbergen, J. G. Snijders, T. Ziegler, *J. Comput. Chem.* **2001**, *22*, 931–967.
[41] C. Fonseca Guerra, J. G. Snijders, G. Velde, E. J. Baerends, *Theor. Chem. Acc.* **1998**, *99*, 391–403.
[42] A. Coenen, *Adv. Chem. Ser.* **1965**, *48*, 76–86.
[43] Bruker APEX2 software, **2016**.
[44] G. M. Sheldrick, *SADABS*, University of Göttingen, Germany, **2008**.
[45] G. M. Sheldrick, *Acta Crystallogr. Sect. A* **2015**, *71*, 3–8.
[46] G. M. Sheldrick, *SHELXL2014*, University of Göttingen, Germany, **2014**.
[47] D. Becke, *Phys. Rev. A.* **1988**, *38*, 3098–3100.
[48] J. P. Perdew, *Phys. Rev. B.* **1986**, *33*, 8822–8824.
[49] E. Van Lenthe, E. J. Baerends, *J. Comput. Chem.* **2003**, *24*, 1142–1156.
[50] A. Grimme, S. Antony, J. Ehrlich, S. Krieg, *J. Chem. Phys.* **2010**, *132*, 154104.

Manuscript received: June 2, 2020
Revised manuscript received: July 13, 2020
Accepted manuscript online: July 13, 2020
Version of record online: September 11, 2020